

Catalytic activities of oxo–Mn–triazacyclononane complexes: spectral studies and single crystal X-ray structure of $[\text{Mn}_4\text{O}_6(1,4,7\text{-triazacyclononane})_4](\text{ClO}_4)_4 \cdot \text{H}_2\text{O}$

T.H. Bennur, D. Srinivas*, S. Sivasanker, V.G. Puranik

Catalysis Division, National Chemical Laboratory, Pune 411008, India

Received 20 March 2004; received in revised form 15 May 2004; accepted 15 May 2004

Abstract

Monomeric terminal-oxo– and tetrameric bridged-oxo–Mn complexes viz., $[(\text{tmtacn})\text{Mn}(\text{O})(\text{H}_2\text{O})]\text{SO}_4$, and $[\text{Mn}_4\text{O}_6(\text{tacn})_4](\text{ClO}_4)_4 \cdot \text{H}_2\text{O}$, respectively, were isolated and characterized by FT-IR, UV–vis, EPR and magnetic susceptibility. Here, tmtacn = *N,N',N''*-trimethyl-1,4,7-triazacyclononane and tacn = 1,4,7-triazacyclononane. Single crystal X-ray structure of the tetrameric bridged-oxo–Mn complex is reported. The catalytic oxidation activities of these complexes for benzylic C–H bond oxidation of ethylbenzene with aqueous H_2O_2 and *tert*-butyl hydroperoxide (TBHP) are reported. The studies reveal that nuclearity and type of oxo–Mn speciation influence the catalytic activity. While the monomeric terminal-oxo–Mn complex exhibits efficient C–H bond oxidation activity, the tetrameric bridged-oxo–Mn complex shows the catalase activity.

© 2004 Elsevier B.V. All rights reserved.

Keywords: Oxo–Mn complexes; Triazacyclononane complexes of Mn; Oxidation of ethylbenzene; Peroxidases; Catalase activity; X-ray structure; Spectroscopic characterization

1. Introduction

Oxo–Mn complexes of varying nuclearity constitute the active sites of manganese-containing metalloenzymes and proteins [1–5]. Specific functionality of these enzymes, in regio- and stereoselective biological transformations, is often, correlated to their unique structure and facile redox properties. It is important, for designing efficient selective oxidation catalysts, to know that how does the activity of oxo species of different nuclearity differ in a specific chemical transformation. We report the catalytic activities of monomeric terminal-oxo–Mn–tmtacn and tetrameric bridged-oxo–Mn–tacn complexes for ethyl benzene (EB) oxidation with H_2O_2 and *tert*-butyl hydroperoxide (TBHP) oxidants. Here, tmtacn = *N,N',N''*-trimethyl-1,4,7-triazacyclononane and tacn = 1,4,7-triazacyclononane.

While the stability, structure, spectroscopy and magnetic properties of peraza macrocyclic complexes have been widely investigated [6,7], only recently, their catalytic activities at ambient temperatures have been reported [8–14]. In situ prepared Mn complexes of tmtacn, in the presence of carboxylate buffers, exhibit efficient catalytic activities in the stereoselective epoxidation of olefins and oxidation of alkanes and alcohols, with H_2O_2 [8–11]. The reactivity of Mn–tmtacn depends on the nature of the carboxylate buffer. It is noteworthy that Mn peroxidases too exhibit such an enhancement in the enzymatic activity in the presence of oxalate and small molecular chelates [2–4]. In the course of understanding the differences in activities of Mn–tmtacn–carboxylate system, we had undertaken spectroscopic investigations [14] and found formation of terminal-oxo– and bridged-oxo–Mn complexes during oxidation reactions. Concentrations of the oxo–Mn species varied with the nature of the carboxylate buffer. Oxalate buffer generates mostly the terminal-oxo while acetate buffer generates the bridged-oxo–Mn complexes. The terminal-oxo–Mn complexes, formed in situ, were proposed

* Corresponding author. Tel.: +91 20 2589 3300; fax: +91 20 2589 3761.

E-mail address: srinivas@cata.ncl.res.in (D. Srinivas).

to be the active Mn species [14]. As an extension to this work, we now establish the proposed hypothesis. Monomeric terminal-oxo-Mn-tmtacn ($[(\text{tmtacn})\text{Mn}(\text{O})(\text{H}_2\text{O})]\text{SO}_4$) and tetrameric bridged-oxo-Mn-tacn ($[\text{Mn}_4\text{O}_6(\text{tacn})_4](\text{ClO}_4)_4 \cdot \text{H}_2\text{O}$) are now synthesized and isolated. Catalytic oxidation activities of these oxo-Mn species of different nuclearity are reported along with their spectroscopic characterizations. Single crystal X-ray structure of the tetrameric bridged-oxo-Mn complex is also reported.

2. Experimental

2.1. Materials

The ligands tacn and tmtacn were prepared by a modified Richmann-Atkin's synthesis method [13]. Spectroscopic characterization confirmed the purity of these ligands. Characterization data of these ligands are as follows:

- 1,4,7-Triazacyclononane (tacn)–
 ^1H NMR (CDCl_3 ; δ ppm): 2.79 (s, 6H), 2.63 (br, 3H);
 IR (Nujol, cm^{-1}): 3306, 2854–2928, 1660, 1458, 1364, 1157, 1032, 997;
 MS: M^+ 126, 112, 99, 85, 73, 56, 44 (base peak).
- 1,4,7-Trimethyl-1,4,7-triazacyclononane (tmtacn)–
 ^1H NMR (CDCl_3 ; δ ppm): 2.38 (s, 9H), 2.70 (s, 12H);
 IR (Nujol, cm^{-1}): 2802–2900, 1666, 1600, 1454, 1373, 1290, 1076, 1031, 999;
 MS: M^+ 171, 154, 147, 127, 115, 99, 84, 70, 58, 42 (base peak).

2.2. Synthesis of oxo-Mn complexes

2.2.1. $[(\text{tmtacn})\text{Mn}(\text{O})(\text{H}_2\text{O})]\text{SO}_4$

The terminal-oxo-Mn complex was prepared from an aqueous solution (2 ml) of MnSO_4 (1 mmol), tmtacn (1 mmol) in methanol (4 ml) and sodium oxalate (1 mmol) dissolved in water (4 ml). The mixture was heated at 313 K, for 2 h, filtered and kept for slow evaporation (2–3 days) to obtain polycrystalline material. Yield: 55% (0.208 g). Anal. Calcd. for $\text{MnC}_9\text{N}_3\text{SO}_6\text{H}_{23}$: C, 30.3; H, 6.5; N, 11.8. Found: C, 30.6; H, 6.4; N, 11.7. Although H_2O_2 was not used in the preparation, aerial oxygen reacted with the Mn(II)-tmtacn solution during the synthesis and isolation, oxidizing it to a terminal-oxo-Mn complex.

2.2.2. $[\text{Mn}_4\text{O}_6(\text{tacn})_4](\text{ClO}_4)_4 \cdot \text{H}_2\text{O}$

The bridged-oxo-Mn complex was prepared by adding aqueous solutions of $\text{Mn}(\text{NO}_3)_2 \cdot 4\text{H}_2\text{O}$ (1.35 mmol; 0.34 g; 2 ml), and sodium oxalate (1.49 mmol, 0.199 g; 4 ml) to a methanolic solution of tacn (1.35 mmol, 0.175 g; 4 ml). The mixture was heated at 333 K for 3 h and to it NaClO_4 (2 mmol; 0.285 g) was added. The pH of the reaction mix-

ture was maintained at 10 using 1 M NaOH. The brown solution obtained was filtered and kept for slow evaporation at 298 K. X-ray quality single crystals were obtained in two days. Yield: 42% (0.175 g). Anal. Calcd. for $\text{Mn}_4\text{Cl}_4\text{O}_{23}\text{N}_{12}\text{C}_{24}\text{H}_{62}$: C, 23.1; H, 5.0; N, 13.5. Found: C, 23.2, H, 5.1; N, 13.5.

Attempts to isolate tetrameric bridged-oxo-Mn-tmtacn and terminal-oxo-Mn-tacn complexes were not successful.

2.3. Characterization studies

Microanalysis of the complexes was done by using a Carlo Erba EA 1108 elemental analyzer. The FT-IR spectra of the Mn complexes (as Nujol mulls) were recorded on a Shimadzu 8201 PC spectrophotometer in the region 400–4000 cm^{-1} . The UV-vis spectra were measured on a Shimadzu UV-2550 spectrophotometer in the region 200–800 nm. The EPR spectra were recorded on a Bruker EMX spectrometer operating at X-band frequency, 100 kHz field modulation, 3 G modulation amplitude and 4 mW microwave radiation power. Frequency calibration was done using a frequency counter fitted in a ER 041 XG-D microwave bridge. Variable temperature experiments were performed on solid polycrystalline samples and CH_3CN solutions by using a Bruker BVT 3000 temperature controller. The g -values and line widths were obtained by spectral simulations using the Bruker Simfonia software package. Magnetic susceptibility measurements (298–77 K) were carried out with a Lewis-coil force magnetometer (Series 300, George Associates, USA). Correction for the diamagnetism was made.

2.4. X-ray crystallographic analysis

Dark brown, thin needle-shaped single crystals grown from a methanolic solution by slow evaporation were used for data collection on a Bruker SMART APEX CCD X-ray diffractometer using Mo $K\alpha$ radiation (50 kV, 40 mA, θ range = 1.02°–22.5°). A summary of the crystal data and structure refinement parameters for the tetrameric bridged-oxo-Mn complex— $2[\text{Mn}_4\text{O}_6(\text{N}_3\text{C}_6\text{H}_{15})_4(\text{ClO}_4)_4 \cdot \text{H}_2\text{O}]$ is given in Table 1. All the data were corrected for Lorentzian, polarization and absorption effects. SHELX-97 [15] was used for structure solution and full matrix least squares refinement on F^2 . Hydrogen atoms were included in the refinement as per the riding model.

There are two molecules of the tetramer having similar conformation, along with eight perchlorate ions and three water molecules (of which two are having half occupancy as a result there are only two water molecules) as a solvent of crystallization in the asymmetric unit. The quality of the crystals is not very good which has resulted in a higher R -value. However, the X-ray structure has been determined unambiguously. Some of the perchlorates are disordered. Crystal structure has been deposited at the Cambridge Crystallographic Data Centre (Deposition No. CCDC 239165).

Table 1

Summary of the crystallographic data and structure refinement parameters for $[\text{Mn}_4\text{O}_6(\text{tmcn})_4](\text{ClO}_4)_4 \cdot \text{H}_2\text{O}$

Empirical formula	$2[(\text{C}_{24}\text{H}_{60}\text{N}_{12}\text{O}_6\text{Mn}_4)(\text{ClO}_4)_4 \cdot \text{H}_2\text{O}]$
Formula weight	2496.83
Temperature	293(2) K
Wavelength	0.71073 Å
Group	P21/n
Unit cell dimensions	
<i>a</i>	24.214(12) Å
<i>b</i>	11.310(6) Å
<i>c</i>	36.080(18) Å
β	91.020(9)°
Volume	9879(9) Å ³
Z, calculated density	4, 1.679 mg/m ³
Absorption coefficient	1.303 mm ⁻¹
<i>F</i> (000)	5136
Crystal size	0.21 mm × 0.13 mm × 0.02 mm
Limiting indices	$-27 \leq h \leq 27, -12 \leq k \leq 12, -41 \leq l \leq 41$
Reflections collected/unique	84077/15485 [<i>R</i> (int) = 0.1663]
Completeness to theta	24.00 (99.9%)
Maximum and minimum transmission	0.9719 and 0.7697
Refinement method	Full-matrix-block least-squares on <i>F</i> ²
Data/restraints/parameters	15485/21/1216
Goodness-of-fit on <i>F</i> ²	0.975
Final <i>R</i> indices [<i>I</i> > 2σ(<i>I</i>)]	<i>R</i> ₁ = 0.0862, <i>wR</i> ₂ = 0.1869
<i>R</i> indices (all data)	<i>R</i> ₁ = 0.1768, <i>wR</i> ₂ = 0.2302
Largest diff. peak and hole	0.773 and -0.498e Å ⁻³

2.5. Catalytic activity and product analysis—oxidation of ethylbenzene

Ethylbenzene (0.5 mmol; 0.053 g) in CH₃CN (1 ml), catalyst (2 μmol) and oxalate buffer (3 μmol; oxalic acid + Na-salt of oxalic acid in 1:1 mol ratio) were taken in a 25 ml double-necked round bottomed glass flask fitted with a water-cooled reflux condenser and placed in an oil bath at 333 K. To it, 38 wt.% aqueous H₂O₂ (0.3 ml, 0.3 mmol) diluted with 0.2 ml CH₃CN was added drop-wise, over a period of 20 min. The reaction was conducted at 333 K and the progress of the reaction was monitored by gas chromatography (Varian 3400 GC; CP-SIL8CB column; 30 m × 0.53 mm). The products formed were identified by GC-MS (Shimadzu QP 5000; DB1 column, 30 m × 0.25 mm) and GC-IR (Perkin Elmer 2000; BP-1 column, 0.25 m × 0.32 mm).

In the experiments with the catalyst system prepared in situ, MnSO₄·H₂O (2 μmol) dissolved in 0.1 ml of water, tmtacn (3 μmol) in 0.1 ml of CH₃CN and oxalate buffer (3 μmol) were taken in the glass reactor placed at 333 K. To it, 0.5 mmol ethylbenzene in 0.8 ml of CH₃CN was added. Then, 0.3 ml of 38 wt.% aqueous H₂O₂ diluted with 0.2 ml of CH₃CN was added over a period of 20 min and the reaction was monitored.

In the experiments with *tert*-butyl hydroperoxide (TBHP) as oxidant, the reactions were performed in a similar manner except that, 1 mmol of ethylbenzene (0.106 g) in 1 ml of acetonitrile, 4 μmol of catalyst and 3 mmol of 70% aqueous TBHP were reacted.

3. Results and discussion

3.1. Spectroscopic and single crystal X-ray structural characterization

3.1.1. FT-IR and UV-vis

In addition to the typical bands due to coordinated tmtacn ligand, the terminal-oxo-Mn complex showed a characteristic, signature band of terminal-oxo at 975 cm⁻¹ [16,17] (Fig. 1, curve B). This band overlaps with those of counter ion SO₄²⁻. The tetrameric complex, on the contrary, showed a well separated, intense, characteristic Mn–O–Mn band at 725 cm⁻¹ [18–20] (Fig. 1; curve A). The in situ prepared catalyst system (from a mixture of MnSO₄, tmtacn, oxalate and H₂O₂ in CH₃CN–water medium) showed the 975 cm⁻¹ band of a terminal-oxo-Mn [9].

The terminal-oxo-Mn complex showed a UV band at about 300 nm possibly attributable to a O → Mn charge transfer transition [16,17] (Fig. 2). Complex 2 showed a prominent band at about 346 nm [18–20]. The in situ prepared system, in fact, showed both these UV bands. The spectral studies, thus, indicate that both these types of oxo-Mn complexes are formed during the reactions with the in situ prepared Mn–tmtacn system.

3.1.2. X-ray structure

A conclusive evidence for the structure was obtained from the single crystal X-ray diffraction studies. An ORTEP view of the complex cation of the bridged-oxo-Mn is shown in Fig. 3. The complex crystallized with two

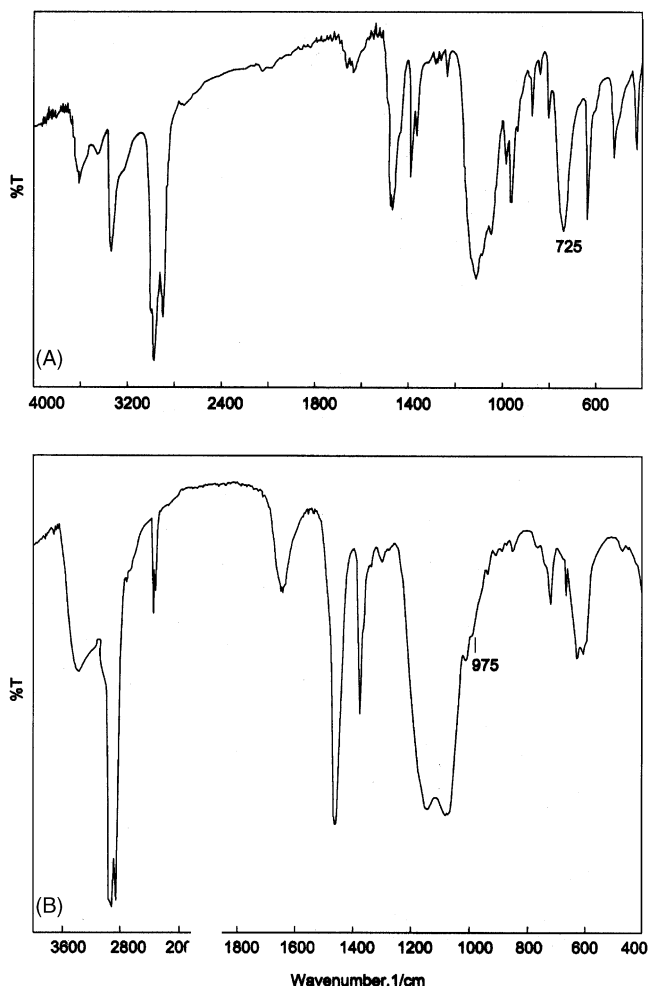


Fig. 1. FT-IR spectra of (A) tetrameric bridged-oxo-Mn ($[\text{Mn}_4\text{O}_6(\text{tacn})_4](\text{ClO}_4)_4 \cdot \text{H}_2\text{O}$) and (B) monomeric terminal-oxo-Mn ($([\text{mntacn}]\text{Mn}(\text{O})(\text{H}_2\text{O}))\text{SO}_4$) complexes. The characteristic bands due to bridged-Mn–O–Mn (at 725 cm^{-1}) and terminal-oxo-Mn (at 975 cm^{-1}) are marked.

tetrameric molecular units having similar conformation, along with four ClO_4^- ions and a water molecule as solvent of crystallization in the asymmetric unit. The Mn_4O_6 core has an adamantane-like skeleton (Fig. 3). The structure of the complex in different crystalline forms ($[\text{Mn}_4\text{O}_6(\text{tacn})_4]\text{ClO}_4$, $\text{Mn}_4\text{O}_6(\text{tacn})_4(\text{ClO}_4)_4 \cdot 2\text{H}_2\text{O}$ and $[\text{Mn}_4\text{O}_6(\text{tacn})_4]\text{Br}_4 \cdot 5\text{H}_2\text{O}$) is already known [18–21]. The Mn atoms occupy the corners of a nearly regular tetrahedron and the connecting oxo-bridges are located above the center of the six edges of this tetrahedron. Each Mn^{4+} ion is in a distorted octahedral environment of three facially coordinated N atoms of tacn ligand and three *cis*- μ -oxo groups. The average Mn–O distance (1.808 Å) is in agreement with that found in the other Mn_4O_6 crystalline forms and is typical for the Mn–O–Mn entities [18–21]. The Mn–N bonds are longer (2.128 Å) due to the *trans*-effect of the strong Mn–O bonds (1.808 Å). The average Mn...Mn distance is 3.25 Å. Selected bond lengths and bond angles of the complex are listed in Table 2. The monomeric

Table 2

Selected bond lengths (Å) and bond angles ($^\circ$) for $[\text{Mn}_4\text{O}_6(\text{tacn})_4](\text{ClO}_4)_4 \cdot \text{H}_2\text{O}$

Molecule 1	Molecule 2
Mn(1)–O(1) 1.797(6)	Mn(5)–O(7) 1.795(6)
Mn(1)–O(5) 1.816(6)	Mn(5)–O(11) 1.803(6)
Mn(1)–O(4) 1.824(6)	Mn(5)–O(10) 1.800(6)
Mn(1)–N(2) 2.121(8)	Mn(5)–N(13) 2.119(8)
Mn(1)–N(3) 2.118(8)	Mn(5)–N(14) 2.121(8)
Mn(1)–N(1) 2.130(8)	Mn(5)–N(15) 2.149(9)
Mn(2)–O(6) 1.790(6)	Mn(6)–O(8) 1.809(6)
Mn(2)–O(2) 1.811(7)	Mn(6)–O(12) 1.805(6)
Mn(2)–O(1) 1.813(7)	Mn(6)–O(7) 1.817(6)
Mn(2)–N(4) 2.113(9)	Mn(6)–N(16) 2.111(8)
Mn(2)–N(5) 2.140(8)	Mn(6)–N(17) 2.120(8)
Mn(2)–N(6) 2.146(9)	Mn(6)–N(18) 2.127(8)
Mn(3)–O(5) 1.794(6)	Mn(7)–O(11) 1.802(6)
Mn(3)–O(2) 1.813(6)	Mn(7)–O(9) 1.809(6)
Mn(3)–O(3) 1.820(6)	Mn(7)–O(8) 1.817(6)
Mn(3)–N(7) 2.126(8)	Mn(7)–N(20) 2.128(8)
Mn(3)–N(9) 2.127(8)	Mn(7)–N(19) 2.127(8)
Mn(3)–N(8) 2.137(9)	Mn(7)–N(21) 2.133(8)
Mn(4)–O(4) 1.805(6)	Mn(8)–O(9) 1.788(6)
Mn(4)–O(6) 1.807(6)	Mn(8)–O(12) 1.807(6)
Mn(4)–O(3) 1.808(6)	Mn(8)–O(10) 1.822(6)
Mn(4)–N(11) 2.118(8)	Mn(8)–N(23) 2.118(8)
Mn(4)–N(10) 2.129(8)	Mn(8)–N(24) 2.120(8)
Mn(4)–N(12) 2.133(8)	Mn(8)–N(22) 2.118(8)
O(1)–Mn(1)–O(5) 98.8(3)	O(7)–Mn(5)–O(11) 98.9(3)
O(1)–Mn(1)–O(4) 98.5(3)	O(7)–Mn(5)–O(10) 99.1(3)
O(5)–Mn(1)–O(4) 98.8(3)	O(11)–Mn(5)–O(10) 99.2(3)
O(1)–Mn(1)–N(2) 88.9(3)	O(7)–Mn(5)–N(13) 167.2(3)
O(5)–Mn(1)–N(2) 166.8(3)	O(11)–Mn(5)–N(13) 90.0(3)
O(4)–Mn(1)–N(2) 90.5(3)	O(10)–Mn(5)–N(13) 88.5(3)
O(1)–Mn(1)–N(3) 88.5(3)	O(7)–Mn(5)–N(14) 89.9(3)
O(5)–Mn(1)–N(3) 88.9(3)	O(11)–Mn(5)–N(14) 165.6(3)
O(4)–Mn(1)–N(3) 168.6(3)	O(10)–Mn(5)–N(14) 90.5(3)
N(2)–Mn(1)–N(3) 80.5(3)	N(13)–Mn(5)–N(14) 79.6(4)
O(1)–Mn(1)–N(1) 165.2(3)	O(7)–Mn(5)–N(15) 91.0(3)
O(5)–Mn(1)–N(1) 89.9(3)	O(11)–Mn(5)–N(15) 89.2(3)
O(4)–Mn(1)–N(1) 91.8(3)	O(10)–Mn(5)–N(15) 165.6(3)
N(2)–Mn(1)–N(1) 80.5(3)	N(13)–Mn(5)–N(15) 79.8(4)
N(3)–Mn(1)–N(1) 79.7(3)	N(14)–Mn(5)–N(15) 79.3(4)
O(6)–Mn(2)–O(2) 98.6(3)	O(8)–Mn(6)–O(12) 98.4(3)
O(6)–Mn(2)–O(1) 98.3(3)	O(8)–Mn(6)–O(7) 99.1(3)
O(2)–Mn(2)–O(1) 99.2(3)	O(12)–Mn(6)–O(7) 98.8(3)
O(6)–Mn(2)–N(4) 87.7(3)	O(8)–Mn(6)–N(16) 168.6(3)
O(2)–Mn(2)–N(4) 168.3(3)	O(12)–Mn(6)–N(16) 89.6(3)
O(1)–Mn(2)–N(4) 89.5(3)	O(7)–Mn(6)–N(16) 87.6(3)
O(6)–Mn(2)–N(5) 166.5(3)	O(8)–Mn(6)–N(17) 90.8(3)
O(2)–Mn(2)–N(5) 91.6(3)	O(12)–Mn(6)–N(17) 166.3(3)
O(1)–Mn(2)–N(5) 88.6(3)	O(7)–Mn(6)–N(17) 89.7(3)
N(4)–Mn(2)–N(5) 80.7(4)	N(16)–Mn(6)–N(17) 80.0(3)
O(6)–Mn(2)–N(6) 90.8(3)	O(8)–Mn(6)–N(18) 91.3(3)
O(2)–Mn(2)–N(6) 89.5(3)	O(12)–Mn(6)–N(18) 89.6(3)
O(1)–Mn(2)–N(6) 166.2(3)	O(7)–Mn(6)–N(18) 165.4(3)
N(4)–Mn(2)–N(6) 80.5(4)	N(16)–Mn(6)–N(18) 80.6(3)
N(5)–Mn(2)–N(6) 80.4(3)	N(17)–Mn(6)–N(18) 80.0(3)
O(5)–Mn(3)–O(2) 98.5(3)	O(11)–Mn(7)–O(9) 98.6(3)
O(5)–Mn(3)–O(3) 99.2(3)	O(11)–Mn(7)–O(8) 99.1(3)
O(2)–Mn(3)–O(3) 99.2(3)	O(9)–Mn(7)–O(8) 98.6(3)
O(5)–Mn(3)–N(7) 90.2(3)	O(11)–Mn(7)–N(20) 165.2(3)
O(2)–Mn(3)–N(7) 89.9(3)	O(9)–Mn(7)–N(20) 89.7(3)
O(3)–Mn(3)–N(7) 165.7(3)	O(8)–Mn(7)–N(20) 91.7(3)
O(5)–Mn(3)–N(9) 88.9(3)	O(11)–Mn(7)–N(19) 89.4(3)

Table 2 (Continued)

Molecule 1	Molecule 2
O(2)–Mn(3)–N(9) 167.1(3)	O(9)–Mn(7)–N(19) 166.6(3)
O(3)–Mn(3)–N(9) 89.9(3)	O(8)–Mn(7)–N(19) 90.7(3)
N(7)–Mn(3)–N(9) 79.5(3)	N(20)–Mn(7)–N(19) 80.3(3)
O(5)–Mn(3)–N(8) 165.2(3)	O(11)–Mn(7)–N(21) 88.3(3)
O(2)–Mn(3)–N(8) 92.0(3)	O(9)–Mn(7)–N(21) 88.8(3)
O(3)–Mn(3)–N(8) 89.3(3)	O(8)–Mn(7)–N(21) 168.6(3)
N(7)–Mn(3)–N(8) 79.4(4)	N(20)–Mn(7)–N(21) 79.6(3)
N(9)–Mn(3)–N(8) 78.9(3)	N(19)–Mn(7)–N(21) 80.6(3)
O(4)–Mn(4)–O(6) 99.4(3)	O(9)–Mn(8)–O(12) 99.2(3)
O(4)–Mn(4)–O(3) 98.0(3)	O(9)–Mn(8)–O(10) 98.6(3)
O(6)–Mn(4)–O(3) 99.3(3)	O(12)–Mn(8)–O(10) 98.0(3)
O(4)–Mn(4)–N(11) 90.7(3)	O(9)–Mn(8)–N(23) 89.0(3)
O(6)–Mn(4)–N(11) 165.1(3)	O(12)–Mn(8)–N(23) 167.2(3)
O(3)–Mn(4)–N(11) 90.0(3)	O(10)–Mn(8)–N(23) 90.3(3)
O(4)–Mn(4)–N(10) 168.4(3)	O(9)–Mn(8)–N(24) 166.9(3)
O(6)–Mn(4)–N(10) 87.8(3)	O(12)–Mn(8)–N(24) 89.3(3)
O(3)–Mn(4)–N(10) 89.7(3)	O(10)–Mn(8)–N(24) 89.9(3)
N(11)–Mn(4)–N(10) 80.6(3)	N(23)–Mn(8)–N(24) 81.0(3)
O(4)–Mn(4)–N(12) 90.8(3)	O(9)–Mn(8)–N(22) 89.5(3)
O(6)–Mn(4)–N(12) 89.2(3)	O(12)–Mn(8)–N(22) 89.9(3)
O(3)–Mn(4)–N(12) 166.5(3)	O(10)–Mn(8)–N(22) 167.6(3)
N(11)–Mn(4)–N(12) 79.7(3)	N(23)–Mn(8)–N(22) 80.4(3)
N(10)–Mn(4)–N(12) 80.2(3)	N(24)–Mn(8)–N(22) 80.6(3)
Mn(1)–O(1)–Mn(2) 128.4(4)	Mn(5)–O(7)–Mn(6) 127.8(3)
Mn(3)–O(2)–Mn(2) 127.7(4)	Mn(6)–O(8)–Mn(7) 127.5(3)
Mn(4)–O(3)–Mn(3) 127.4(3)	Mn(8)–O(9)–Mn(7) 128.6(4)
Mn(4)–O(4)–Mn(1) 127.6(4)	Mn(5)–O(10)–Mn(8) 127.8(3)
Mn(3)–O(5)–Mn(1) 128.1(3)	Mn(5)–O(11)–Mn(7) 128.1(3)
Mn(2)–O(6)–Mn(4) 128.7(4)	Mn(8)–O(12)–Mn(6) 128.4(3)

terminal-oxo-Mn did not yield good quality single crystals and hence, its X-ray structure could not be determined. Earlier, Shul'pin et al. [10,11] isolated a dimeric tri(μ -oxo)-Mn-tmtacn complex and reported its catalytic activity in hydrocarbon oxidations. Based on these results it can be concluded that different types of oxo-Mn com-

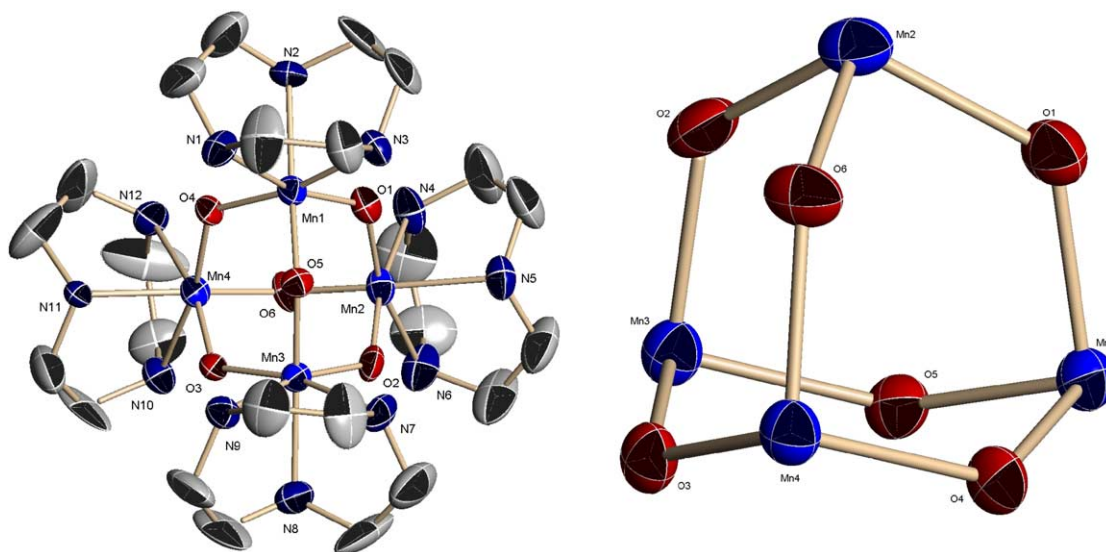


Fig. 3. ORTEP view (left) and core picture (right) of complex cation of $\text{Mn}_4\text{O}_6(\text{tacn})_4(\text{ClO}_4)_4 \cdot \text{H}_2\text{O}$. Ellipsoids are drawn at 40% probability.

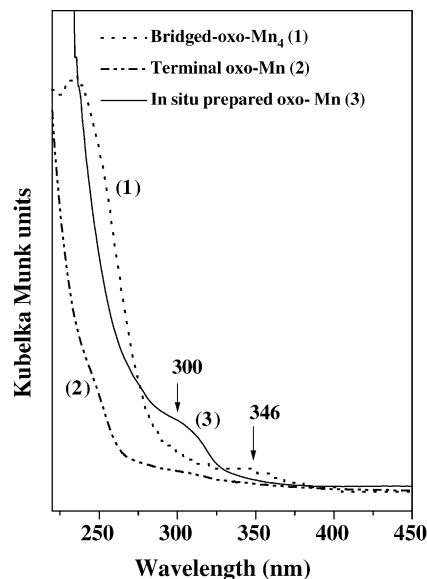


Fig. 2. UV-vis spectra in $\text{CH}_3\text{CN-H}_2\text{O}$ mixture: (1) tetrameric bridged-oxo-Mn ($[\text{Mn}_4\text{O}_6(\text{tacn})_4][\text{ClO}_4]_4 \cdot \text{H}_2\text{O}$) + oxalate + H_2O_2 , (2) monomeric terminal-oxo-Mn ($[(\text{tmtacn})\text{Mn}(\text{O})(\text{H}_2\text{O})]\text{SO}_4$) + oxalate + H_2O_2 . (3) In situ prepared Mn-tmtacn-oxalate- H_2O_2 system. Charge transfer bands due to bridged-oxo-Mn (at 346 nm) and terminal-oxo-Mn (at 300 nm) are indicated.

plexes are formed during the course of reaction, as shown in Fig. 4.

3.1.3. EPR spectroscopy and magnetic susceptibility

Polycrystals of terminal-oxo-Mn were paramagnetic and showed an intense EPR signal ($g_{\text{iso}} = 2.0$, $\Delta H_{\text{pp}} = 148 \text{ G}$). Mn hyperfine features were not resolved. A weak signal at $g = 4.2$ was observed at higher spectrometer gain indicating a +4 oxidation state for Mn. The tetrameric complex showed a broad signal ($\Delta H_{\text{pp}} = 618 \text{ G}$) whose intensity increased and line width decreased with lowering of the

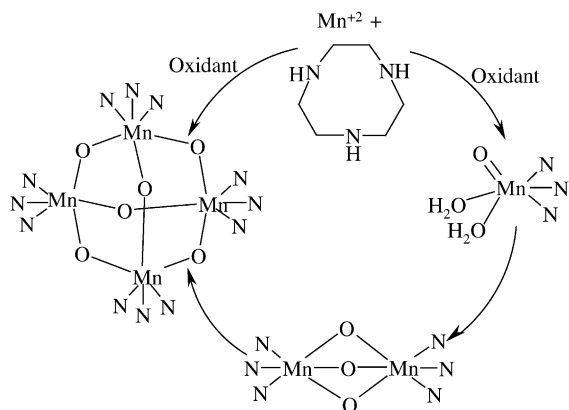


Fig. 4. Oxo-Mn species of different nuclearity in the reaction mixture.

temperature (Fig. 5). The EPR spectra of the latter complex are consistent with weak intramolecular ferromagnetic interactions between Mn ions. This was further confirmed by performing magnetic susceptibility measurements in the temperature range 298–77 K. A plot of $1/\chi_M$ versus T (best fitted to the exchange Hamiltonian, $H_{ex} = \sum_{i>j} -J_{ij}S_iS_j$, assuming a d^3 electron configuration for the four Mn(IV) centers) (Fig. 6) yielded an exchange coupling constant, J , of $14.2 \pm 0.3 \text{ cm}^{-1}$. This value agrees well with the reports on Mn_4O_6 -type cationic core complexes [18–21]. The spec-

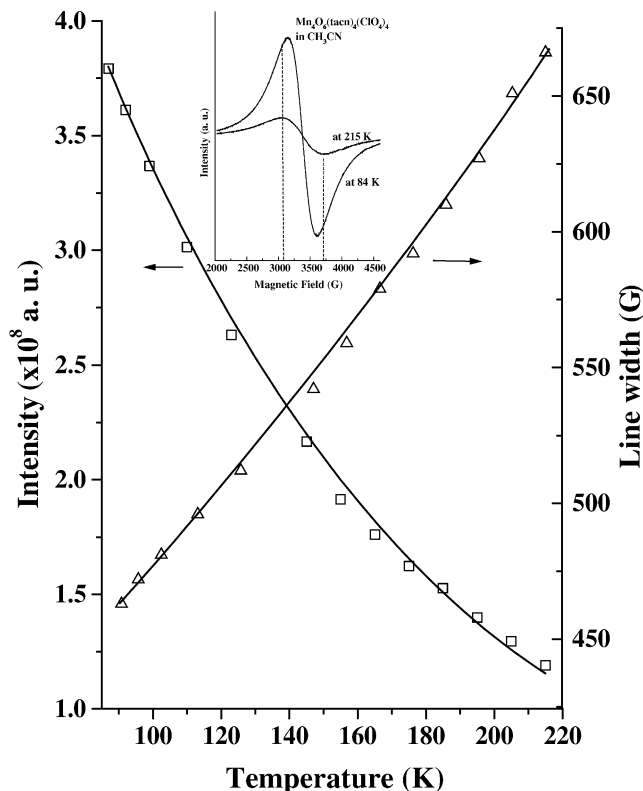


Fig. 5. Variation of EPR signal intensity and linewidth of tetrameric bridged-oxo-Mn complex as a function of temperature. Inset shows the EPR spectra at 215 and 84 K.

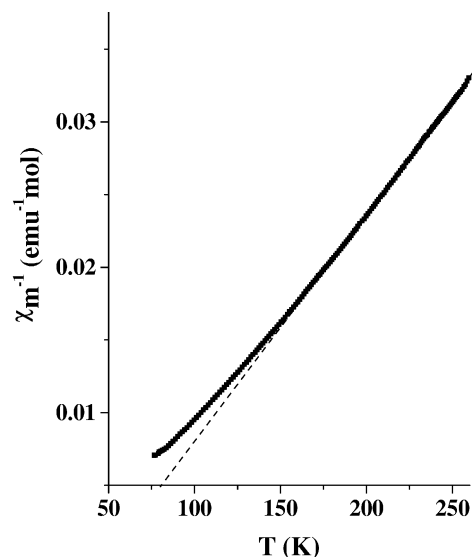


Fig. 6. Variable temperature magnetic susceptibility data of $[\text{Mn}_4\text{O}_6(\text{tacn})_4](\text{ClO}_4)_4 \cdot \text{H}_2\text{O}$.

tral and structural characterization study confirms the formation and integrity of the terminal-oxo- and bridged-oxo-Mn species.

3.2. Catalytic activity studies

Catalytic activities of the monomeric terminal-oxo-Mn, tetrameric bridged-oxo-Mn and in situ prepared Mn-tmtacn system in the presence of oxalate buffer for benzylic C–H bond oxidation of ethylbenzene (EB) with H_2O_2 (38% aqueous) are reported in Table 3. 1-Phenylethanol and acetophenone were the benzylic oxidation products. *Ortho*- and *para*-ring hydroxylated products were also observed. β -C–H bond oxidation was not detected. In the absence of oxalate buffer EB conversion was negligible (1.5 in 0.5 h; turnover number (TON) = 4). A plot of EB conversion with reaction time for the in situ prepared Mn complex and isolated, monomeric terminal-oxo-Mn complex (Fig. 7) indicates that the activities of these systems are similar in the initial 0.5 h. Later on, the in situ prepared system shows lower activity than the terminal-oxo-Mn complex. Interestingly, the tetranuclear bridged-oxo-Mn complex, exhibits no activity (Table 3). It simply decomposed H_2O_2 into $\text{H}_2\text{O} + \text{O}_2$. In other words, while the monomeric terminal-oxo-Mn complex exhibits efficient the oxygenase activity, the tetranuclear bridged-oxo complex exhibits the catalase activity. This indicates that specific oxidation activity depends on the nuclearity and type of oxo-Mn species. Lower activity of the in situ prepared complex (beyond 0.5 h) is due to formation of bridged-oxo-Mn clusters from the active terminal-oxo-Mn species as shown in Fig. 4. In the initial 0.5 h the reaction mixture contains predominantly the terminal-oxo-Mn^{IV} complexes. During the course of time, the reactive terminal-oxo-Mn oligomerizes in the presence of Mn(II) ions present in the in situ reaction mix-

Table 3
Catalytic activity data of oxo-Mn-triazacyclononane complexes in ethylbenzene (EB) oxidation^a

Catalyst	Buffer	Oxidant	Reaction time (h)	EB conversion (wt.%)	TON ^b	Benzylic product selectivity (wt.%) ^c
In situ prepared Mn-tmtacn complex	–	H ₂ O ₂	0.5	1.5	4	32.6
	Oxalate	H ₂ O ₂	0.5	27.0	68	57.3
			4	42.3	104	60.3
[(tmtacn)Mn(O)(H ₂ O)]SO ₄	Oxalate	H ₂ O ₂	1	38.4	96	67.5
			4	50.6	128	57.6
[Mn ₄ O ₆ (tacn) ₄](ClO ₄) ₄ ·H ₂ O	Oxalate	H ₂ O ₂	4	0	0	0
[(tmtacn)Mn(O)(H ₂ O)]SO ₄	Oxalate	TBHP	1	37.4	93	90.9
			4	59.4	148	96.9
			10	98.5	246	97.6
[Mn ₄ O ₆ (tacn) ₄](ClO ₄) ₄ ·H ₂ O	–	TBHP	10	26.4	66	76.9
	Oxalate	TBHP	10	83.3	208	94.3

^a See Section 2 for reaction conditions.

^b Turnover number (TON) = moles of EB converted per mole of catalyst.

^c Combined selectivity of 1-phenylethanol and acetophenone. Rest are ring hydroxylated products.

ture into inactive tetrameric bridged-oxo-Mn complexes. This structural transformation poisons the catalytic activity of the in situ prepared system.

When TBHP, instead of H₂O₂, was used a complete conversion of EB (98.5% with 95% benzylic selectivity) was obtained, in 10h, over the terminal-oxo-Mn complex (Fig. 7). The tetrameric bridged-oxo-Mn complex also showed a good activity in the presence of oxalate buffer (EB conversion = 83.3%, benzylic selectivity = 94.3%). In the absence of oxalate, EB conversion over the bridged-oxo-Mn complex was only 26.4% (benzylic selectivity = 76.9%). The present study reveals that nuclearity of the oxo-Mn species plays a key role on their catalytic oxidation activity. Stabilization of these oxo-Mn species of different type and

nuclearity by encapsulating them in the cages of zeolite molecular sieves or polymeric matrices can possibly enable designing efficient, biomimetic catalysts with specific oxidation functionality. In the mechanism of peroxide dismutation it has been proposed that H₂O₂ is initially activated by coordinating through both of its oxygen atoms to two metal centers (μ_2 -type coordination) of an active complex, which is followed by a homolytic O–O cleavage and further conversion into H₂O and O₂ [22,23]. With the cluster complexes of present type (having a bulky ligand like tacn) it is difficult to form such a TBHP–metal complex intermediate species and hence, its decomposition is not possible. On the contrary, smaller peroxides like H₂O₂ can be decomposed.

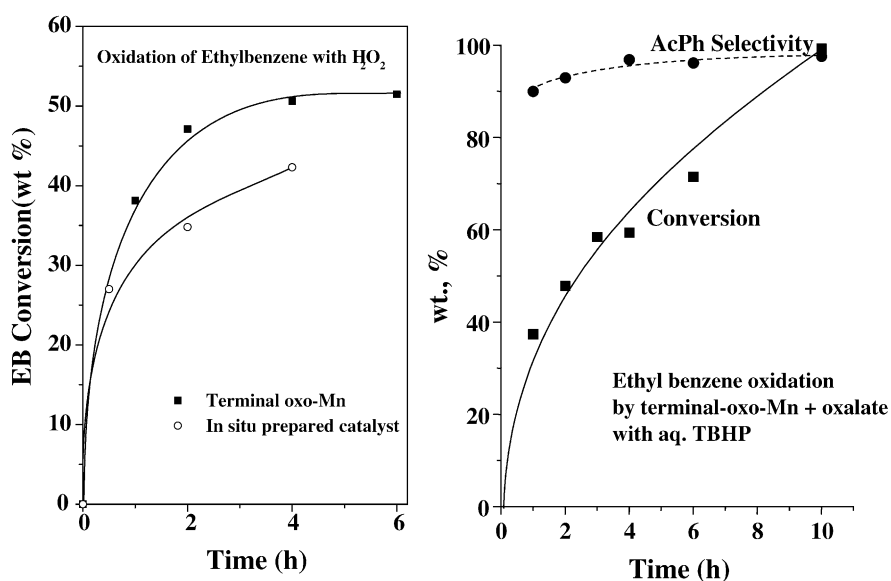


Fig. 7. Left: catalytic activities of terminal-oxo-Mn-tmtacn and in situ prepared Mn-tmtacn complexes for ethylbenzene oxidation in the presence of oxalate buffer with H₂O₂ as oxidant. Right: catalytic activity of terminal-oxo-Mn complex in ethylbenzene oxidation using *tert*-butyl hydroperoxide at 333 K.

Our attempts to isolate oxalate coordinated oxo–Mn–triazacyclononane complexes are so far not successful in spite of the fact that buffer is used in the synthesis. This suggests that the bonding of oxalate to the Mn system is labile. Table 3 reveals that oxalate buffer not only enhances the catalytic activity but also the benzylic product selectivity. Differences in product selectivity (benzylic versus ring hydroxylated products) are noted also when TBHP instead of H₂O₂ is used as oxidant. Benzylic product is formed in greater amounts with TBHP than with H₂O₂.

4. Conclusions

The catalytic oxidation activities of monomeric terminal-oxo–Mn and tetrameric bridged-oxo–Mn complexes ([tmtacn]Mn(O)(H₂O)]SO₄, and [Mn₄O₆(tacn)₄](ClO₄)₄·H₂O, respectively) for benzylic C–H bond oxidation of ethylbenzene with aqueous H₂O₂ and *tert*-butyl hydroperoxide (TBHP) are investigated. The studies reveal that the nuclearity and type of oxo–Mn speciation influence the catalytic oxidation activity. While the monomeric terminal-oxo–Mn complex exhibits efficient C–H bond oxidation activity, the tetrameric bridged-oxo–Mn complex shows only the catalase activity when H₂O₂ was the oxidant. This difference in activity of oxo–Mn complexes is not significant when TBHP instead of H₂O₂ was used.

Acknowledgements

D.S. thanks Department of Science and Technology, New Delhi for financial support. T.H.B. acknowledges CSIR, New Delhi for the award of senior research fellowship.

References

- [1] B. Meunier (Ed.), Metal–oxo and Metal–peroxo Species in Catalytic Oxidations, Structure and Bonding, vol. 97, Springer-Verlag, Berlin, 2000.
- [2] V.L. Pecoraro, Mn-redox Enzymes, VCH Publishers, New York, 1992.
- [3] (a) M.T. Candle, V.L. Pecoraro, Adv. Inorg. Chem. 46 (1999) 305; (b) G. Christou, Acc. Chem. Res. 22 (1989) 328.
- [4] L. Que, A.E. True, Prog. Inorg. Chem. 38 (1990) 97.
- [5] K. Wieghardt, Angew. Chem. Int. Ed. Eng. 28 (1989) 1153.
- [6] P. Chaudhuri, K. Wieghardt, Prog. Inorg. Chem. 35 (1987) 329.
- [7] K.P. Wainwright, Coord. Chem. Rev. 166 (1997) 35.
- [8] D.E. De Vos, T. Bein, J. Organomet. Chem. 195 (1996) 520.
- [9] D.E. De Vos, S. de Wildeman, B.F. Sels, P.J. Grobet, P.A. Jacobs, Angew. Chem. Int. Ed. Eng. 38 (1999) 980.
- [10] J.R.L. Smith, G.B. Shul'pin, Tetrahedron Lett. 39 (1998) 4909.
- [11] G.B. Shul'pin, G. Suss-Fink, L.S. Shul'pin, J. Mol. Catal. A: Chem. 170 (2001) 17.
- [12] C. Zondervan, R. Hage, B.L. Feringa, Chem. Commun. (1997) 419.
- [13] T.H. Bennur, D. Srinivas, S. Sivasanker, J. Mol. Catal. A: Chem. 207 (2004) 163.
- [14] T.H. Bennur, S. Sabne, S.S. Deshpande, D. Srinivas, S. Sivasanker, J. Mol. Catal. A: Chem. 185 (2002) 71.
- [15] G.M. Sheldrick, SHELX-97 Program For Crystal Structure Solution and Refinement, University of Gottingen, Germany, 1997.
- [16] J.T. Groves, Y. Watanabe, Inorg. Chem. 25 (1986) 4808.
- [17] T.J. Collins, R.D. Powell, C. Slebodwick, E.S. Uffeleman, J. Am. Chem. Soc. 112 (1990) 897.
- [18] K. Wieghardt, U. Bossek, W. Gebert, Angew. Chem. Int. Ed. Eng. 22 (1983) 328.
- [19] K. Wieghardt, D. Ventur, Y.H. Tsai, C. Krüger, Inorg. Chim. Acta 99 (1985) L25.
- [20] K. Wieghardt, U. Bossek, B. Nuber, J. Weiss, J. Bonvoisin, M. Cornbella, S.E. Vitols, J.J. Girerd, J. Am. Chem. Soc. 110 (1988) 7398.
- [21] K.S. Hagen, T.D. Westmoreland, M.J. Scott, W.H. Armstrong, J. Am. Chem. Soc. 111 (1989) 1907.
- [22] Y. Sasaki, T. Akamatsu, K. Tsuchiya, S. Ohba, M. Sakamoto, Y. Nishida, Polyhedron 17 (1998) 235.
- [23] J. Gao, S.H. Zhong, J. Mol. Catal. A: Chem. 186 (2002) 25.